HTML ABSTRACT + LINKS

Near-field-enhanced, mold-assisted, parallel direct nanostructuring of a gold thin film on glass

D. B. Shao, S. F. Li, and S. C. Chen[a)]
Department of Mechanical Engineering, University of Texas at Austin, Austin, Texas 78712

(Received 30 July 2004; accepted 14 October 2004)

In this report, near-field enhancement around nanoridges and nanotips upon 532 nm pulsed laser irradiation is utilized to produce line or dot pattern on gold thin films deposited on glass substrates. The ridges and tips, which have end radii on the order of 50 nm, were fabricated out of silicon dioxide thin film on silicon by microfabrication techniques. A 30 nm chromium thin film was evaporated onto the ridges or tips by e-beam evaporation to enhance the near-field effect. Line and dot array were successfully patterned on the Au film with feature size ranging from 100 to 200 nm. Results from numerical simulation using finite difference time domain method agree with experimental results. © *2004 American Institute of Physics*. [DOI: 10.1063/1.1828239]

The aggressive pursuit of ever decreasing feature size in modern integrated circuit fabrication has been a hallmark of the microelectronics industry. Finer feature size is not only desirable in microelectronics for higher performance, but also in nanomanufacturing for applications in biomedical engineering and life sciences. However, it is difficult to achieve critical dimensions at subwavelength scale due to the optical diffraction limit using traditional lithography techniques. Recently the optical near-field effect has been utilized to achieve smaller feature sizes since the near-field effect itself is a phenomenon at the subwavelength scale.[1–5] Although different approaches have been developed in designing near-field masks, a common problem is that the field enhancement is usually small and as a result, the produced features are usually not well defined.

On the other hand, the strong near-field enhancement around nanotips has been widely studied for the purpose of near-field scanning optical microscopy (NSOM).[6,7] The finite difference time domain (FDTD) method has been employed to investigate the factors that influence field enhancement including polarization of incident radiation, angle of incidence, tip size, and materials. Numerical simulation of a gold tip in water has indicated that an optical enhancement factor of 3000 was achieved when laser illumination is perpendicular to the tip axis, but barely any enhancement was observed when laser incidence is along the tip axis.[7] Previous work also concluded that metallic and semiconductor materials tend to produce higher near-field enhancement. This near-field phenomenon around the nanotip has been used for direct nanopatterning when the tips were placed close to a substrate. Lines of 14 nm in width were produced on gold using a single atomic force microscopy (AFM) tip made of silicon.[8] The laser irradiation was incident from the side, perpendicular to the tip axis since it is believed that only the electric field component along the tip axis plays an important role in near-field enhancement. However, a systematic numerical study has indicated that the maximum enhancement may occur when incidence is with an angle.[9]

It has been our goal to achieve large area parallel patterning utilizing the near-field effect. In this letter the strong field enhancement adjacent to nanotips are extended to the use of nanoridges to produce line features. Following the microfabrication techniques used to make a tip array,[10] long rectangular masks were used to fabricate ridge array by isotropic etching. The first layer, 4-μm-thick low temperature oxide, was deposited on a silicon wafer using low pressure chemical vapor deposition (LPCVD). The wafer was then annealed at 1000 °C for about an hour to enhance film density and etching durability. Then a layer of 200 nm polysilicon mask for buffered oxide etching (BOE) was deposited by LPCVD, followed by a second mask layer of 100 nm aluminum for reactive ion etching. 20:1 BOE was used to slow down the etching process for better control. The tips or ridges formed right after the masks were etched free. Finally, the ridges and the tips were coated with a 30 nm layer of chromium by e-beam evaporation. Figure 1 shows the scanning electron microscopy (SEM) image of the ridges, which has end radii on the order of 50 nm.

As shown in Fig. 2, a gold film of 25 nm thickness was deposited on a Pyrex substrate by electron beam evaporation. Laser irradiation (full width half maximum = 10 ns, wavelength = 532 nm) was from the back of the substrate at an angle of about 50°, with polarization indicated in the figure. The thickness of the film was chosen so that significant local field enhancement can be generated. A two-dimensional TM mode FDTD code was developed to calculate the field enhancement for different configurations. To verify the accuracy of the program, the code was benchmarked with the

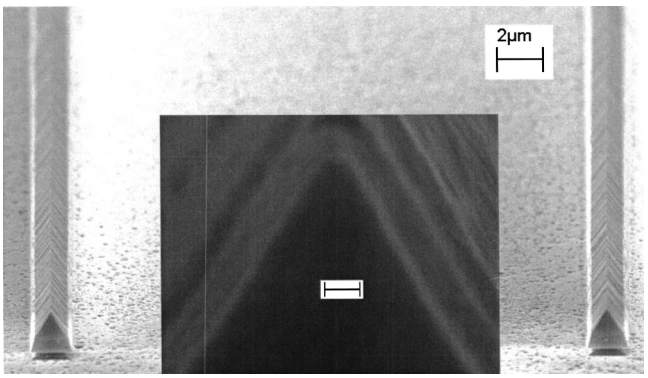

FIG. 1. SEM pictures of ridge array on the nanomold used in the experiment. The scale bar in the inset indicates 100 nm.

[a)]Electronic mail: scchen@mail.utexas.edu

 © 2004 American Institute of Physics

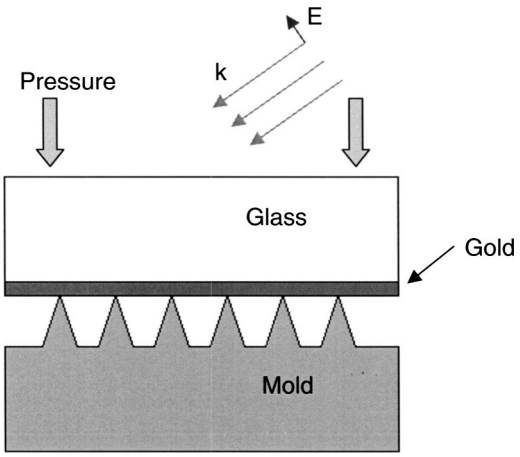

FIG. 2. A schematic view of the experimental setup.

two-dimensional theoretical solutions of the scattering of light by a cylinder.[11] The optical properties of the materials were first determined[12] and fitted with the Drude model,[13] and were then input to the code. Figure 3(a) shows the contour of the electric field around the contacting area between the ridge and the substrate. The numerical value along the line A–A as indicated in Fig. 3(a) was extracted and plotted in Fig. 3(b). The results show maximum energy enhancement of ~11 is achievable with this configuration.

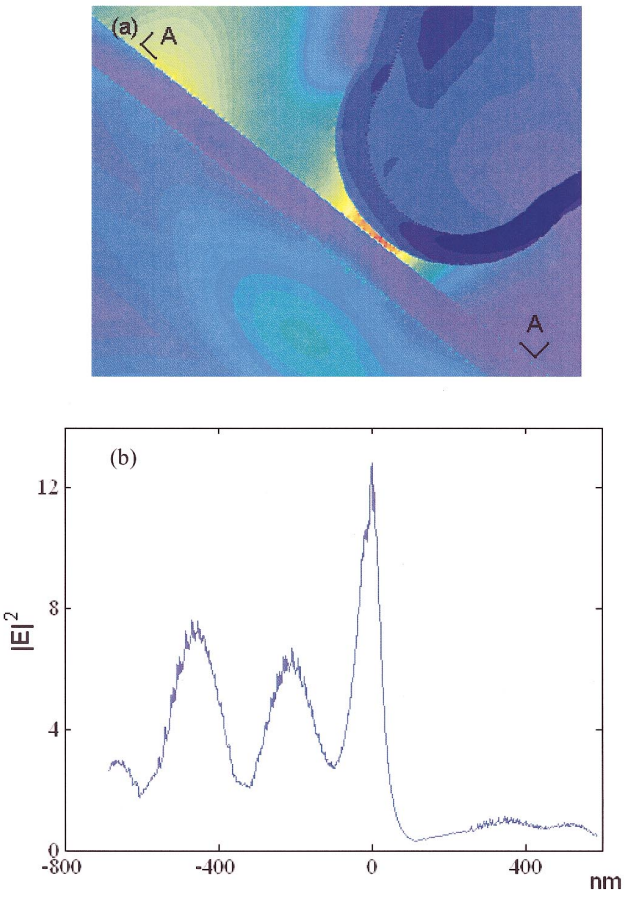

FIG. 3. (Color) FDTD simulation results: (a) contour plot of electric field amplitude distribution in the vicinity of the ridge end (radius 50 nm) and the substrate, (b) the electric field amplitude on the surface of the glass substrate along cross-section A–A. The near-field enhanced peak has a width of about 100 nm at the half peak value.

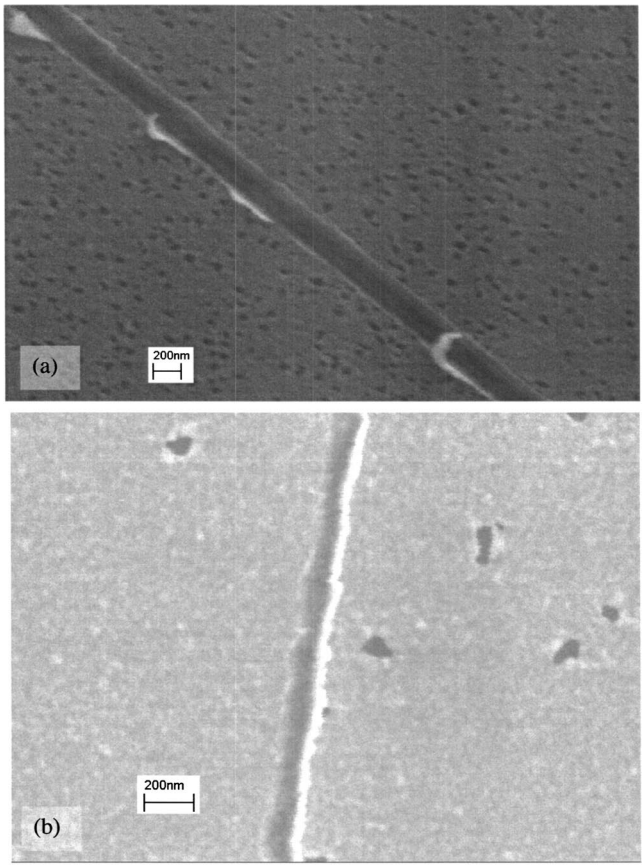

FIG. 4. SEM close view of the line pattern at laser energy of (a) 0.26 J/cm^2, (b) 0.20 J/cm^2.

Before the experiment, the threshold laser intensity for direct ablation of the gold film without the near-field mold was first measured as ~0.53 J/cm^2 at the incident angle of 50° of laser irradiation. The laser energy was then reduced by a factor of 2–3 for direct patterning using the near-filled mold. To ensure contact between the ridges and the glass substrate, a small force was applied during the experiment.

The SEM images in Fig. 4 show that lines were successfully transferred to the gold film on glass from the ridges of the near-field mold. The pattern size and quality were affected by the laser energy used. At half the threshold energy (~0.26 J/cm^2), the width of the lines were measured to be about 200 nm, as shown in Fig. 4(a). In this case, the features are well defined and smooth at the boundary. When the laser energy were lowered to about 0.20 J/cm^2, the feature size decreased to about 100 nm; however the defects of the ridges, result of the defects of the etching mask made by E-beam lithography, became noticeable on the patterns [Fig. 4(b)]. AFM results revealed pattern depth of ~20 nm for the high energy case, as seen in Fig. 5, and about 15 nm for the low intensity case. By using a tip array instead of ridge array, an array of pits was produced on the gold thin film, as shown in Fig. 6, at about 1/4 of the threshold energy, since the tip structure has stronger optical field enhancement compared to that of a ridge.

From Fig. 4 the residue of the gold film can be observed at the edges of the channels or pits. AFM results shown in Fig. 5 also verified this. Even though the pressing force between the mold and the sample might have played a role in the patterning process, direct molding without laser incidence did not create any pattern on the gold film. Further-

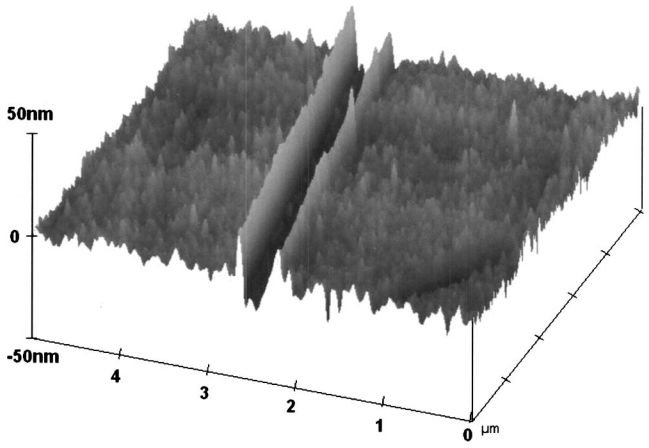

FIG. 5. AFM results of the line pattern at laser energy of 0.26 J/cm^2.

more, for the same laser energy and pressing force, simply rotating the ridge array horizontally by 90 degree with respect to the incidence laser beam resulted in no pattern formation, which indicates the angle dependence of the near-field effect.

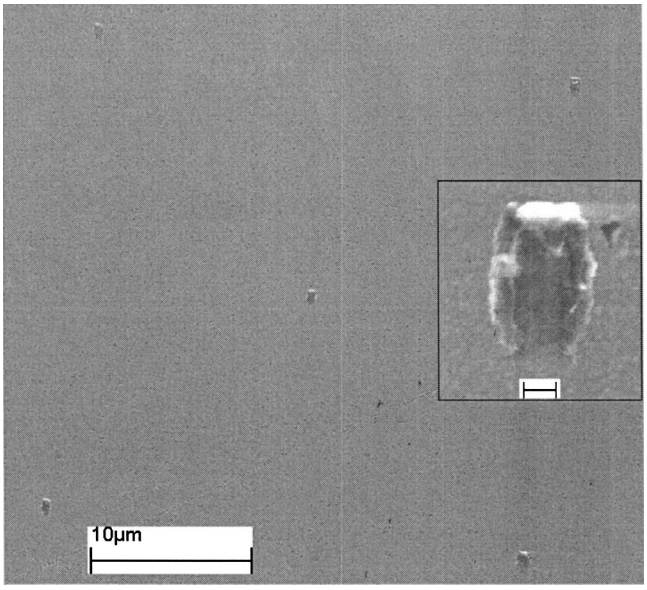

FIG. 6. SEM images dot array on a gold film. The scale bar in the inset indicates 200 nm.

The laser intensity enhancement factor (<3) by the ridge structure from the experiment was much smaller than the predicted value (~ 11) from FDTD simulation. The discrepancies can be understood by considering the pinholes of the evaporated gold film and defects at the interface, which will scatter incident laser radiation and reduce laser intensity coming to the contacting area. By improving the quality of the metallic film, higher enhancement could be achieved in experiment and as a result, the width and the quality of the patterns can be controlled better by adjusting the laser energy.

In summary, nanomold assisted near-field enhanced patterning technique is used to produce feature sizes down to 100 nm on a metallic film on a transparent glass substrate. This process can be highly parallel by using array of ridges or tips to write line array or dot array, respectively. By improving the mask film quality and refining the ridges or tips of the near-field mold, this method might generate even smaller feature sizes.

The authors would like to thank Professor Li Shi and Dr. Stephen Gray for helpful discussion. This work was supported by research grants from the U.S. National Science Foundation (DMI 0222014 and CTS 0243160).

[1]J. G. Goodberlet and H. Kavak, Appl. Phys. Lett. **81**, 1315 (2002).
[2]R. Riehn, A. Charas, J. Morgado, and F. Cacialli, Appl. Phys. Lett. **82**, 526 (2003).
[3]H. Schmid, H. Biebuyck, B. Michel, and O. J. F. Martin, Appl. Phys. Lett. **72**, 2379 (1998).
[4]R. Kunz, M. Rothschild, and M. S. Yeung, J. Vac. Sci. Technol. B **21**, 78 (2003).
[5]S. Theppakuttai and S. C. Chen, Appl. Phys. Lett. **83**, 758 (2003).
[6]J. T. Krug II, E. J. Sanchez, and X. S. Xie, J. Chem. Phys. **116**, 10895 (2002).
[7]L. Novotny, R. X. Bian, and X. S. Xie, Phys. Rev. Lett. **79**, 645 (1997).
[8]A. Chimmalgi, T. Y. Choi, C. P. Grigoropoulos, and K. Komvopoulos, Appl. Phys. Lett. **82**, 1146 (2003).
[9]W. X. Sun and Z. X. Shen, J. Opt. Soc. Am. A **20**, 2254 (2003).
[10]L. Shi, O. Kwon, A. C. Miner, and A. Majumdar, J. Microelectromech. Syst. **10**, 370 (2001).
[11]P. W. Barber and S. C. Hill, *Light Scattering by Particles: Computational Methods* (World Scientific, Singapore, 1990).
[12]E. D. Palik, *Handbook of Optica1 Constants of Solids* (Academic, Orlando, FL, 1985).
[13]S. K. Gray and T. Kupka, Phys. Rev. B **68**, 045415 (2003).